molecular pharmaceutics

articles

Polymer Nanoparticles for Immunotherapy from Encapsulated Tumor-Associated Antigens and Whole Tumor Cells

C. M. Solbrig,[†] J. K. Saucier-Sawyer,[†] V. Cody,[‡] W. M. Saltzman,*[,†] and D. J. Hanlon[‡]

Departments of Biomedical Engineering and Dermatology, Yale University, New Haven, Connecticut 06520-8260

Received October 5, 2006; Revised Manuscript Received December 13, 2006; Accepted December 15, 2006

Abstract: Encapsulation of tumor-associated antigens (TAA) in polymer nanoparticles is a promising approach to increasing the efficiency of antigen (Ag) delivery for antitumor vaccines. We optimized a polymer preparation method to deliver both defined tumor-associated proteins and the complex mixtures of tumor Ags present in tumors. Tumor Ags were encapsulated in a biodegradable, 50:50 poly(D,L-lactide co-glycolide) copolymer (PLGA) by emulsification and solvent extraction. Two particular Ags were studied, gp100 (a melanoma-associated antigen) and ovalbumin (OVA), as well as mixtures of proteins and lysates of tumor cells. The efficiency of encapsulation was measured by protein assays of dissolved nanoparticles. Ag stability after release from nanoparticles was verified by SDS−acrylamide gel electrophoresis and Western blot analysis. Molecular weight and protein loading interact to define the encapsulation efficiency and release rate of nanoparticles formulated from 50:50 PLGA. A midrange molecular weight polymer had more desirable release properties at 100 mg/mL than at 50 mg/mL protein loading, indicating the need for optimization of nanoparticle formulation for preparations with different particle loadings. Mixtures of proteins derived from cell lysates were reliably encapsulated into nanoparticles, which released the spectrum of proteins contained in lysates. Antigenic proteins were co-encapsulated with cell lysate and released from nanoparticles; these Ags retained their antigenicity and functioned better than soluble Ags when tested in in vitro assays of T cell cytokine formation and in vivo tumor vaccination challenge.

Keywords: Nanoparticle; PLGA; antigen delivery; B16 melanoma; cell lysates

Introduction

Current antitumor vaccine strategies, based predominantly on the loading of professional antigen-presenting cells, such as dendritic cells (DC), with tumor-associated antigens, have proven to be partially effective in a limited number of malignancies in which tumor-associated antigens have been characterized.[1] However, the small number of defined TAA for most categories of solid tumors has limited extension of these studies to common malignancies. In the absence of defined Ags, an autologous tumor is an attractive source of antigenic material; autologous tumor cells also contain the full panoply of tumor Ags relevant to that particular person. One possible approach is to derive tissue culture lines for feeding or fusing to DC,[2] but this approach may not mirror the antigenicity of the original tumor. In addition, this technique has proven to be time-consuming and laborious to apply to most tumors. Alternatively, a protein lysate can be made directly from the tumor, thereby maximizing the spectrum of tumor Ags present, and this soluble mixture can

* Corresponding author: Yale University, P.O. Box 208260, New Haven, CT 06520-8260. For express delivery: 55 Prospect Street, 413 Malone Engineering Center, New Haven, CT 06511. Phone: 203-432-4262. Fax: 203-432-0030. E-mail: mark.saltzman@yale.edu.

[†] Department of Biomedical Engineering.

[‡] Department of Dermatology.

(1) Mocellin, S.; Mandruzzato, S.; Bronte, V.; Lise, M.; Donato, N. Part I: Vaccines for solid tumours. *Lancet Oncol.* **2004**, *5*, 681−689.

(2) Gong, J. Immunotherapy of cancer based on DC-tumor fusion vaccine. *Curr. Immunol. Rev.* **2006**, *2* (3), 291−304.

10.1021/mp060107e CCC: $37.00
Published on Web 01/12/2007

be fed to DC. But this methodology also has its drawbacks, since it is well-established that soluble macromolecules are inherently less stable in solution and poorly internalized by phagocytes like DC.

We explored an alternative technology that appears to transfer Ag to DC with high efficiency. In a recent study, encapsulation of a single protein Ag, ovalbumin, in biodegradable polymer nanoparticles was shown to increase the amount of Ag presented by DCs, apparently by facilitating the endosomal escape of encapsulated Ag within DC and high-efficiency MHC class I presentation.[3] On the basis of these results, we reasoned that encapsulation of an Ag-loaded cell lysate could also produce enhanced stimulation of Ag-specific antitumor T cells, provided the tumor lysate can be encapsulated with high efficiency and reliably released. To test this hypothesis, we have used this technology, termed "nanoparticle-mediated tumor delivery", to encapsulate both defined tumor Ags and whole tumor lysates chosen from a well-defined murine tumor, B16 melanoma, that contains a known TAA, gp100.

Encapsulation of purified proteins in biodegradable polymers has been studied extensively;[4,5,6,7] however, only a few previous studies have examined the encapsulation of cellular material,[8,9] and no studies of which we are aware use encapsulated tumor material. In developing this approach, we assumed two features are important to engineer into any potential whole cell-based system for activation of DC. First, we desire delivery of Ags over a sustained period of approximately 7 days, which is roughly the functional time span for DC antigen presentation. We achieved this aim by manipulating the formulation of nanoparticles, which involves variables such as polymer molecular weight, initial protein loading, and stabilizer concentration. Second, we want to ensure a representative selection of proteins from the cells are efficiently encapsulated and released from the particles. To evaluate these factors, we prepared nanoparticles from a single protein OVA, a combination of proteins [bovine serum albumin (BSA), OVA, and lysozyme (LYS)], and freeze−thaw (FT) lysates of B16 melanoma cells. We characterized the particles in terms of protein encapsulation, release, and biological activity.

Methods

Individual Antigens. OVA (Sigma, St. Louis, MO) was used as a 5 or 10% (w/v) solution in phosphate-buffered saline (PBS) (Invitrogen, Carlsbad, CA). Fluorescein 5-isothiocyanate (FITC)-labeled OVA (Molecular Probes, Carlsbad, CA) was used in some experiments. GP100 was obtained through genetic expression of a vector grown in *Escherichia coli* that produced a GST fusion protein; the protein was prepared by E. Feshchenko and was a gift from M. P. Weiner. OVA and gp100 were also co-encapsulated with B16 melanoma cell lysate preparations; a known amount of OVA or gp100 was added to the lysate preparation. OVA was also encapsulated in mixtures with LYS (USB Corp., Cleveland, OH) and BSA (Sigma); in this three-protein preparation, OVA, LYS, and BSA solutions contained equal amounts (by weight) of each protein.

Cell Formulations Used in Lysate Preparation. Lysates were made from the B16.F10 cell line (ATCC, Manassas, VA) directly recovered from cell culture flasks or from tumors produced by implantation of B16.F10 cells into the flanks of female C57BL/6 mice (Jackson Laboratory, Bar Harbor, ME). In culture, cells were grown to 95% confluency. Tumors were grown subcutaneously in mice, surgically resected, and minced so they could be dissociated into single-cell monolayers. Tumor lysates were produced from either 80×10^6 cells or an equivalent number of cells liberated from growing tumors. Cells were resuspended in 250 μL of sterile PBS and maintained on ice prior to lysate preparation.

Freeze−Thaw Lysate Preparation. A protein fraction was liberated from the B16.F10 cells and the dissociated tumor fragments by multiple freeze−thaw (FT) incubations. B16.F10 cells (80×10^6) were resuspended in 250 μL of sterile PBS, aliquoted into cryotubes, and subjected to four freeze−thaw cycles with alternating liquid nitrogen−37 °C water bath treatment to break the cell membrane. Cell death and lysis were confirmed by the inability to exclude trypan blue. Lysates were then spun at 12 000 rpm for 15 min at 4 °C to remove cellular debris. The supernatants were collected and stored at −20 °C until they were used.

Octyl β-Glucoside Lysate Preparation. As an alternative means of preparing lysates, B16.F10 cells were solubilized briefly with the dialyzable detergent octyl β-glucoside (OG) (Pierce Chemicals, Rockford, IL) (43 mM) for 30 min followed by removal of the surfactant by dialysis in 200 volumes of PBS, as recommended by the manufacturer.

(3) Shen, H.; Ackerman, V.; Cody, V.; Giodini, A.; Hinson, E. R.; Cresswell, P.; Edelson, R. L.; Saltzman, W. M.; Hanlon, D. J. Enhanced and prolonged cross-presentation following endosomal escape of exogenous antigens encapsulated in biodegradable nanoparticles. *Immunology* **2006**, *117*, 78−88.

(4) Wong, H. M.; Wang, J. J.; Wang, C. H. In vitro sustained release of human immunoglobulin G from biodegradable microspheres. *Ind. Eng. Chem. Res.* **2001**, *40*, 933−948.

(5) Jiang, G.; Woo, B. H.; Kang, F.; Singh, J.; DeLuca, P. P. Assessment of protein release kinetics, stability and protein polymer interaction of lysozyme encapsultaed poly(D,L-lactide-co-glycolide) microspheres. *J. Controlled Release* **2002**, *79*, 137−145.

(6) Sohier, J.; Vlugt, T. J. H.; Cabrol, N.; Van Blitterswijk, C.; de Groot, K.; Bezemer, K. M. Dual release of proteins from porous polymeric scaffolds. *J. Controlled Release* **2006**, *111*, 95−106.

(7) Park, T. G.; Lu, W.; Crotts, G. Importance of in vitro experimental conditions on protein release kinetics, stability and polymer degradation in protein encapsulated poly(D,L-lactic acid-co-glycolic acid) microspheres. *J. Controlled Release* **1995**, *33*, 211−222.

(8) Murillo, M.; Grillo, M. J.; Rene, J.; Marin, C. M.; Barberan, M.; Goni, M. M.; Blasco, J. M.; Irache, J. M.; Gamazo, C. A *Brucella ovis* antigenic complex bearing (poly-ϵ-caprolactone) microparticles confer protection against experimental brucellosis in mice. *Vaccine* **2001**, *19*, 4099−4106.

(9) Ren, J. M.; Zou, Q. M.; Wang, F. K.; He, Q.; Chen, W.; Zen, W. K. PELA microspheres loaded *H. pylori* lysates and their mucosal immune response. *World J. Gastroenterol.* **2002**, *8* (6), 1098−1102.

PLGA Nanoparticle Fabrication. PLGA nanoparticles were fabricated using the solvent evaporation method[10] from a water/oil/water ($W_2/O/W_1$) emulsion.[11] Nanoparticles were created by emulsification of an organic polymer solution and an aqueous solution, resulting in small droplets of polymer that solidify into nanoparticles upon drying. The basic fabrication protocol, which was modified as described in the text to optimize Ag encapsulation, was as follows. PLGA samples with the following characteristics were used: 50:50 (50% lactide and 50% glycolide), inherent viscosity (iv) of 0.59 dL/g (80K Da), iv of 0.39 dL/g (45K Da), and iv of 0.17 dL/g (15K Da); PLGA-COOH, iv of 0.67 (105K Da) (all obtained from DURECT Corp., Pelham, AL). Two hundred milligrams of PLGA was weighed into a glass test tube and dissolved in 2 mL of dichloromethane (Fisher Scientific). To the organic solution was added 200 μL of the protein solution in PBS to be encapsulated which formed a water-in-oil (O/W_1) emulsion. The aqueous protein solution in most cases was characterized by knowing the type of protein that was used, in the case of defined proteins, or the total protein content (determined by protein assay) for the cell lysates. Cell lysates were further characterized by polyacrylamide gel electrophoresis to ascertain the MW distribution of proteins contained in the lysate (see below). In the case of the nanoparticles containing lysates spiked with FITC-labeled OVA, the aqueous protein mixture was prepared as follows. Fifty microliters of a 22 mg/mL solution of FITC-OVA was added to a solution of 185 μL of FT lysate at 55 mg/mL followed by vortexing to ensure a homogeneous solution. The protein was added dropwise as the polymer solution was vortexed. The resultant emulsion was then sonicated three times for 10 s (Tekmar sonicator, micro probe) on ice at a 38% amplitude. This first emulsion was then added dropwise into a solution of poly(vinyl alcohol) (PVA) (concentration either 5% or 0.5%) (Sigma) in a glass test tube while the mixture was being continuously vortexed. This second emulsion, a $W_2/O/W_1$ emulsion, was also sonicated. After sonication, the second emulsion was poured into a beaker containing 100 mL of 0.3% PVA and stirred with a stir bar for 3 h to evaporate dichloromethane. The nanoparticle slurry was then portioned into four 50 mL plastic centrifuge tubes and centrifuged at 12 000 rpm for 40 min to sediment the nanoparticles. After the supernatant was removed, the nanoparticles were washed three successive times with 10 mL of water, resuspending the nanoparticles with each wash. After the last wash, the resultant nanoparticles were combined into one tube and the nanoparticles were resuspended in 5 mL of water and frozen at −80 °C before being lyophilized.

(10) Santos-Sanchez, A. Formulation, in vitro characterization and in vivo evaluation of a biodegradable campthothecin sustained release delivery system for intratumoral treatments of breast cancer. Ph.D. Thesis. Cornell University, Ithaca, NY, 2004.

(11) Cohen, S.; Yoshioka, T.; Lucarelli, M.; Hwang, L. H.; Langer, R. Controlled delivery systems for proteins based on poly(lactic/glycolic acid) microspheres. *Pharm. Res.* **1991**, *8* (6), 713−720.

Table 1. Diameters of Polymer Nanoparticles Obtained from Combinations of 45K and 80K MW Polymer and 5 or 0.5% PVA Stabilizer[a]

nanoparticle (PLGA MW and % PVA)	nanoparticle diameter (nm)
80K and 5%	197 ± 78
80K and 0.5%	211 ± 98
45K and 5%	115 ± 82
45K and 0.5%	287 ± 151

[a] For determination of the average and standard deviation, the sample size was 100 nanoparticles. The PVA concentration had a statistically significant effect on nanoparticle diameter with the 45K polymer (*t* test, $p = 1.39 \times 10^{-6}$), but not for the 80K polymer (*t* test, $p = 0.256$). Nanoparticles were significantly smaller when made with the 80K polymer instead of the 45K polymer if the PVA stabilizer was used at a concentration of 0.5% (*t* test, $p = 4.49 \times 10^{-5}$). No difference in size was seen when 5% PVA was used (*t* test, $p = 0.772$).

Nanoparticle Characterization. Scanning electron microscopy (SEM) and image analysis software (Image J) were employed to measure the diameters and distribution of polymer nanoparticles. Nanoparticles were deposited onto a metal stub on top of a piece of adhesive carbon tape and coated with a thin layer of gold for visualization by SEM. Images were collected at 20000× magnification and analyzed with the Image J imaging program; a representative sampling of nanoparticle diameters ($n = 100$) was recorded and analyzed for each treatment (Table 1).

Assessment of Nanoparticle Protein Encapsulation. To evaluate the encapsulation efficiency of the nanoparticle formation process, the amount of protein released upon dissolution of a predetermined mass of nanoparticles was determined. Nanoparticles (5−10 mg) were degraded overnight at 37 °C in 1 mL of 1 M NaOH (Ricca Chemicals, Arlington, TX). The concentration of the protein released from the single protein particles in Table 2 was determined by measuring the absorbance of the protein at 290 nm and comparing it to a standard curve prepared from known concentrations of the same protein. The concentrations of protein in microparticles containing lysates and made from single proteins in Table 3 were measured with a colorimetric protein assay. The dissolved nanoparticle solution in alkali was neutralized with an equal volume of 1 M HCl (Aldrich, Steinheim, Germany) and the amount of protein measured using a bicinchoninic acid (BCA) assay (BCA Assay Kit, Pierce; $\lambda = 562$ nm, Molecular Probes plate reader). Protein concentrations were determined by comparing absorbance readings to a standard curve generated by the BCA method.

To obtain a solution of encapsulated protein for analysis by polyacrylamide gel electrophoresis (PAGE), several milligrams of particles was dissolved in 0.5 mL of dichloromethane in a microcentrifuge tube. The dichloromethane solution was then extracted four times with 0.2 mL of PBS. The PBS aliquots were added after the nanoparticles had dissolved, and the contents of the microtube were vortexed to ensure good contact between the immiscible liquids. The PBS extracts were combined, concentrated with a microcon filter concentrator, and loaded onto a gel. Bis-Tris, 4−12%

Table 2. Comparison of Protein Encapsulation and Release by Polymer Particles with Varying Molecular Weights[a]

[OVA] loaded (mg/mL)	PLGA MW	OVA encapsulated (μg/mg)	%EE	OVA burst release (μg/mg)	OVA release at 14 days (μg/mg)	released/encapsulated (%)
50	15K	14	27	0.6	1.2	8.1
50	45K	12	22	1.4	2.1	18
50	80K	27	55	2.6	3.2	12
50	105K	49	99	5.5	9.1	18
100	15K	8.6	8.6	0.9	2.2	26
100	45K	29	29	2.8	7.6	26
100	80K	30	28	1.9	4.6	15
100	105K	32	32	6.3	9.3	29

[a] Nanoparticles were produced with a PLGA polymer varying in size from 15K to 105K. Note that the OVA concentration in the first emulsion, which was either 50 or 100 mg/mL, corresponded to loadings of either 50 or 100 μg/mg (protein/polymer), respectively. The encapsulation efficiency (%EE) was calculated from the formula (mass protein encapsulated in nanoparticles/mass protein loaded) $\times$ 100%. OVA burst and release were assessed over 14 days of incubation of 20 mg of nanoparticles in PBS. The 105K PLGA sample contained carboxyl end groups.

Table 3. Characterization of the Loading and Release of Defined Proteins in 80K MW 50:50 PLGA Nanoparticles[a]

protein encapsulated	protein released at 14 days (μg/mg)	protein encapsulated (μg/mg)	%EE	released/encapsulated (%)
BSA	10	11	~100	90
OVA	1.5	9	90	17
LYS	12	10	100	117
BSA/OVA/LYS	11	11	37	101

[a] Protein loading was 10 mg/mL for BSA, LYS, or OVA nanoparticles and 30 mg/mL for BSA/OVA/LYS nanoparticles.

gradient acrylamide gels (NuPAGE SDS/PAGE, Bis-Tris, Invitrogen) were used to separate the proteins according to molecular weight. Protein molecular weight standards (Benchmark, Invitrogen) were used to determine the relative molecular weights of the proteins. Gels were stained with the Silver *Xpress* Silver Staining Kit (Invitrogen) to visualize the protein bands. Simply Blue Safe Stain (Invitrogen) was used to visualize protein bands on filter blots.

Measurement of the Nanoparticle Protein Release Rate. The rate of release of protein from nanoparticles was measured during incubation under controlled conditions. A sample of nanoparticles (5 mg for multiprotein particles, 10 mg of lysate particles, or 20 mg for OVA particles) was suspended in 2 mL of PBS and incubated at 37 °C with agitation. Periodically, the suspension was centrifuged to pellet the spheres; the supernatant was collected and stored at −20 °C. The spheres were then resuspended in 2 mL in the original tube for another sampling at a later time point. Supernatant samples were analyzed for total protein using the BCA total protein assay, and the cumulative amount of protein released as a function of time was calculated.

Lysate Composition and Protein Integrity. The relative composition of proteins in the different lysate preparations, before and after encapsulation in polymer nanoparticles, was monitored by SDS−PAGE as described above. Samples of protein were concentrated using Centricon YM-10 or Microcon (Millipore, Billerica, MA) filtration units.

Determination of the Antigenicity of Released Protein via Western Blot Assays. In some cases, after separation by PAGE, the proteins were transferred to a nitrocellulose membrane using an electroblotting system [ILNP transfer buffer (20×), nitrocellulose membranes, 0.2 μm, Invitrogen]. The membrane was then probed with antibodies for a primary antigen [anti-chicken, egg albumin (Sigma) for OVA detection; anti-MBP−HRP for gp100 detection], detected with a secondary antibody conjugated to horseradish peroxidase, and detected by the ECL method (GE Healthcare, Buckinghamshire, U.K.).

Cytometric Bead Array. Confirmation of the effectiveness of nanoparticle-mediated Ag delivery was established in experiments utilizing the melanoma-associated protein gp100. The protein content of each formulation was determined, and murine DC were loaded with nanoparticles and used as stimulators for antigen-specific T cells.[3] Murine bone marrow-derived dendritic cells (BMDC) were loaded for 6 h with equimolar quantities of recombinant gp100 protein or B16 FT lysates spiked with gp100, either in soluble form or encapsulated in PLGA particles. These DC were mixed with gp100-specific naïve CD8+ T cells isolated from the spleens of *pmel* transgenic mice [TCR transgenic mice with 95% $gp100_{(25-33)}$-specific, H-$2K^d$-restricted splenic CD8+ T cells].[12] Following coculture of the cells for 24 h, the supernatants were removed and analyzed for production of cytokines associated with DC/T cell stimulation (IL-2 and IFNγ) according to the manufacturer's instructions using a mouse Th1/Th2 cytometric bead array (CBA) cytokine kit (BD Biosciences Pharmingen, San Diego, CA). The use of a cytometric bead array system allowed efficient characterization of T cell stimulation in terms of both the identity of

(12) Overwijk, W. W.; Theoret, M. R.; Finkelstein, S. E.; Surman, D. R.; DeJong, L. A.; Vyth-Dreese, F. A.; Dellemijn, T. A.; Antony, P. A.; Spiess, P. J.; Palmer, D. C.; Heimann, D. M.; Klebanoff, C. A.; Yu, Z.; Hwang, L. N.; Feigenbaum, L.; Kruisbeek, A. M.; Rosenberg, S. A.; Restifo, N. P. Tumor regression and autoimmunity after reversal of a functionally tolerant state of self-reactive CD8+ T cells. *J. Exp. Med.* **2003**, *198* (4), 569−580.

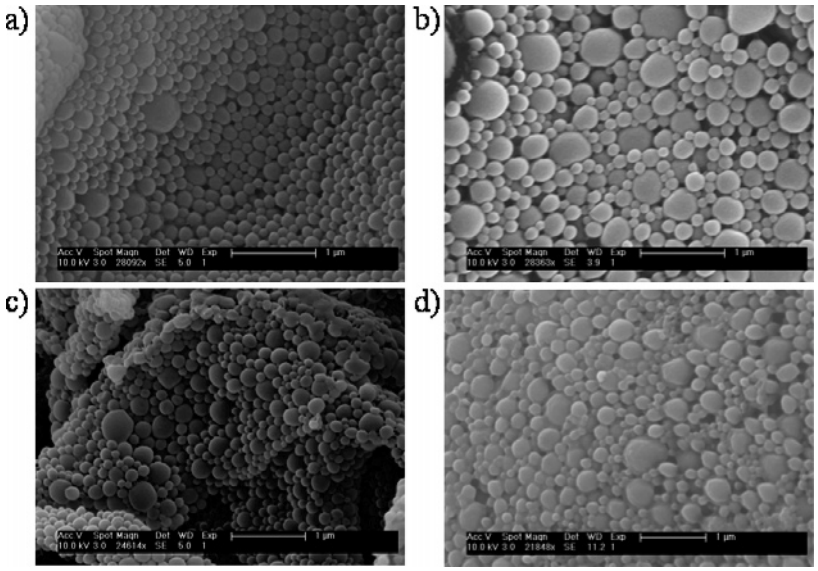

Figure 1. Polymer nanoparticles made with various 50:50 PLGA molecular weights and stabilizer concentrations: (a) 45K with 5% PVA, (b) 45K with 0.5% PVA, (c) 80K with 5% PVA, and (d) 80K with 0.5% PVA.

the multiple cytokines expressed and their individual concentrations, but we recognize that it is only a partial evaluation of a complex response. Blank PLGA nanoparticles were used as a control to rule out the possibility of nonspecific stimulation by PLGA nanoparticles by molecules such as endotoxins and lipopolysaccharides.

Monitoring in Vivo DC Stimulation of Antitumor T Cell Responses. The efficiency of delivery of Ag to DC was compared in vivo in a tumor protection−rejection assay utilizing the murine B16 melanoma model, the model most frequently utilized in evaluating Ag delivery in DC-based vaccination protocols.[13] Using this model, bone marrow-derived DC were loaded ex vivo with equimolar quantities of various Ag sources (soluble Ag preparations or nanoparticle-encapsulated Ag preparations), and then these DC were injected intradermally (ID) into C57BL/6 mice as a cellular vaccine. Treatment groups, consisting of eight mice each, were given two identical vaccinations (5×10^5 DCs), with the second vaccination occurring 14 days after the initial one. The mice were then challenged subcutaneously (sc) 10 days after the second vaccination in the opposite flank with a dose of B16 tumor (1×10^5 cells) known to lead to tumor formation in 100% of unprotected animals. Mean tumor growth and increased survival duration were monitored as a measure of DC vaccination efficiency (and therefore of Ag delivery and cross presentation to DC). The animals were sacrificed as soon as one of the following conditions occurred: either the tumors reached a specific volume (100 mm^2) or the tumors become ulcerated and the animals showed signs of "distress." Because of this experimental constraint, animal numbers were small at late times in the study, making it difficult to assign error bars.

(13) Dranoff, G.; Jaffee, E.; Lazenby, A.; Golumbek, P.; Levitsky, H.; Brose, K.; Jackson, V.; Hamada, H.; Pardoll, D.; Mulligan, R. C. Vaccination with irradiated tumor-cells engineered to secrete murine granulocyte-macrophage colony-stimulating factor stimulates potent, specific, and long-lasting antitumor immunity. *Proc. Natl. Acad. Sci. U.S.A.* **1993**, *90* (8), 3539−3543.

Results

Protein Encapsulation and Release: Defined Protein Preparations. Four molecular weights (MW) of 50:50 PLGA were used to make nanoparticles containing OVA. In all cases, spherical nanoparticles with a range of diameters, from 100 to 300 nm, were obtained (Figure 1 and Table 1). In these initial experiments, we used two different concentrations of PVA as a stabilizer (0.5 and 5%). The higher stabilizer concentration produced smaller nanoparticles from the 45K MW polymer, but not the 80K MW polymer (Table 1). Except where noted below, all other studies employed 5% PVA.

Previous studies suggest that nanoparticle properties depend on two key parameters: the concentration of protein in the loading solution and the polymer molecular weight. Therefore, we fabricated particles from OVA, varied these parameters, and measured the efficiency of encapsulation and the rate of OVA release (Table 2). To characterize the quantity of OVA at each stage of encapsulation and release, we define the following terms: "loaded", the protein preparation prior to exposure to the double-emulsion process; "encapsulated", the protein extracted from the particles after encapsulation, but before controlled release; and "released", the protein released from the particles into aqueous medium during constant incubation.

The fraction of OVA encapsulated (%EE) increased as the MW of the polymer used to make the nanoparticles increased (Table 2). This general trend was noted for both protein loadings. The lower protein loading provided the most substantial increase in %EE with polymer MW (Table 2). All of the formulations released a substantial amount of encapsulated protein, varying from 8 to 29%, during the first 14 days of incubation in PBS. In addition, all of the

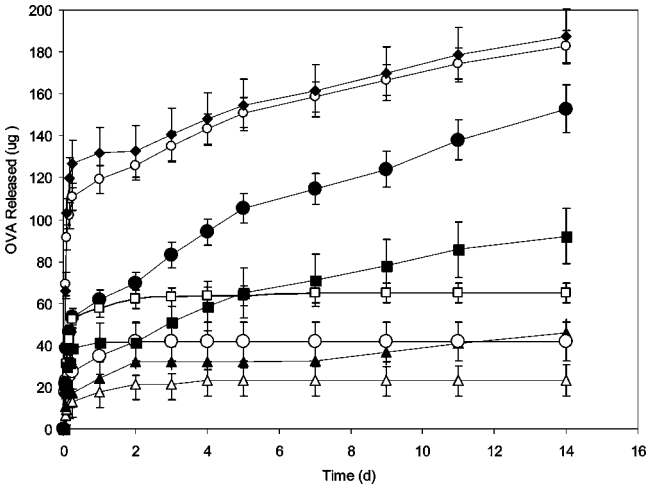

Figure 2. Release as a function of time for a 20 mg sample of nanoparticles of different MW 50:50 PLGA with either 50 mg/mL (empty symbols) or 100 mg/mL (filled symbols) OVA protein in the water phase: 15K (△ or ▲), 45K (○ or ●), 80K (□ or ■), and 105K (with carboxylated endgroups) (○ or ◆). Error bars represent the standard deviation of the mean.

formulations released OVA in two phases: a burst phase of the first 6 h and a sustained phase that lasted up to the entire 14 day period of our experiment. The amount of OVA released during the burst phase, the amount released over 14 days, and the shape of the release curve depended on the MW of PLGA and the initial protein loading (Table 2 and Figure 2). The rate of release (i.e., the slope of the release vs time curve) during the sustained release phase was similar for all MW particles. However, the duration of this phase of release was substantially longer for the 45K, 80K, and 105K MW PLGA nanoparticles than for the 15K MW PLGA nanoparticles, particularly for the higher protein loading (Figure 2). Nanoparticles produced with 105K MW 50:50 PLGA with carboxylated end groups released the most protein after 14 days and exhibited the two-phase release curve at both protein concentrations.

To examine the effect of multiple proteins on encapsulation and release, a mixture of three proteins (BSA, OVA, and LYS) was encapsulated into nanoparticles; the characteristics of these nanoparticles were compared to those of nanoparticles made with each protein individually. The encapsulation efficiency of the individual proteins was more than 2 times higher than the encapsulation efficiency of the protein encapsulated as a mixture (Table 3); this observation follows the general trend noted with OVA particles that %EE decreases with total protein loading (Table 2). Because of the lower encapsulation efficiency of the particles with three proteins, all four nanoparticle preparations contained approximately the same mass of encapsulated protein (between 9 and 11 μg of protein/mg of polymer). These nanoparticles were incubated in PBS for a 14 day period: all of the encapsulated protein was released in 14 days for the BSA, LYS, and BSA/OVA/LYS particles, but the OVA nanoparticles released only 17% of the encapsulated protein (Table 3). The shapes of the release curves for the BSA, OVA, and

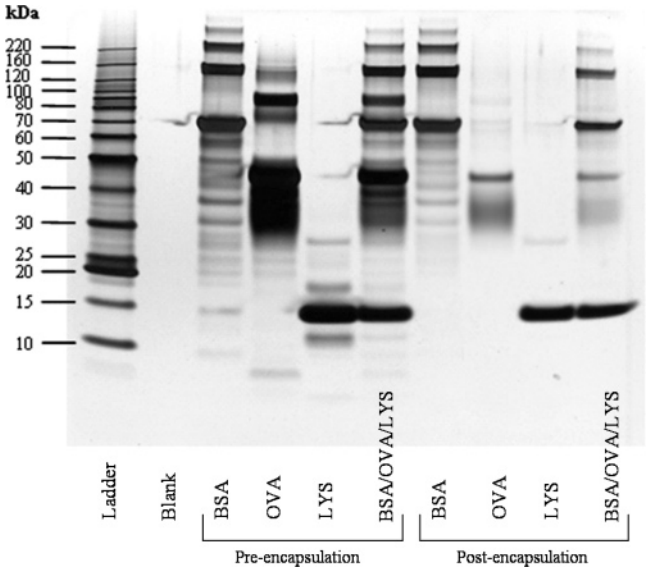

Figure 3. Proteins released from nanoparticles before and after encapsulation in 80K PLGA with a 5% PVA stabilizer. Lane 1 contained a protein ladder. Individual proteins were loaded with 2 mg/mL protein. Combination protein nanoparticles were loaded with 6 mg/mL total protein. Loaded protein before encapsulation: lane 3, BSA; lane 4, OVA; lane 5, LYS; and lane 6, BSA/OVA/LYS. Loaded protein after release from nanoparticles: lane 7, BSA; lane 8, OVA; lane 9, LYS; and lane 10, BSA/OVA/LYS.

LYS nanoparticles were similar; all of the protein was released after 2 days. The BSA/OVA/LYS nanoparticles exhibited more gradual release over a span of 6 days. This observation follows the general trend noted in that the sustained release phase was extended for particles with higher total protein loading.

The loaded and released proteins were analyzed by SDS−PAGE (Figure 3). Some of the higher-molecular weight protein bands, which were present as contaminants in BSA, OVA, and LYS preparations, were not observed in the BSA/OVA/LYS mixture released from the nanoparticles. Furthermore, the intensity of the released OVA band, which was released from nanoparticles that contained the same amount of protein, was reduced compared to those of the bands produced by released BSA and LYS. When the OVA band was released from the nanoparticles containing all three proteins, the intensity was also reduced.

Protein Encapsulation and Release: Cell Lysate Preparations. We used freeze−thaw (FT) methods to produce proteins from cultured B16 cells for loading into nanoparticles. In some cases, we added a dialyzable detergent (OG) during the lysate preparation. When the distribution of protein bands from a FT preparation was compared to that of a preparation with OG, the banding patterns were similar (Figure 4a, lanes 2 and 3): the lysate produced with addition of OG had prominent bands at 130K, 75K, 65K, 55K, 40K, 25K, and 13K, while the FT lysate had prominent bands at 130K, 40K, 27K, 25K, 22K, and 13K and a large band spanning 55−75K.

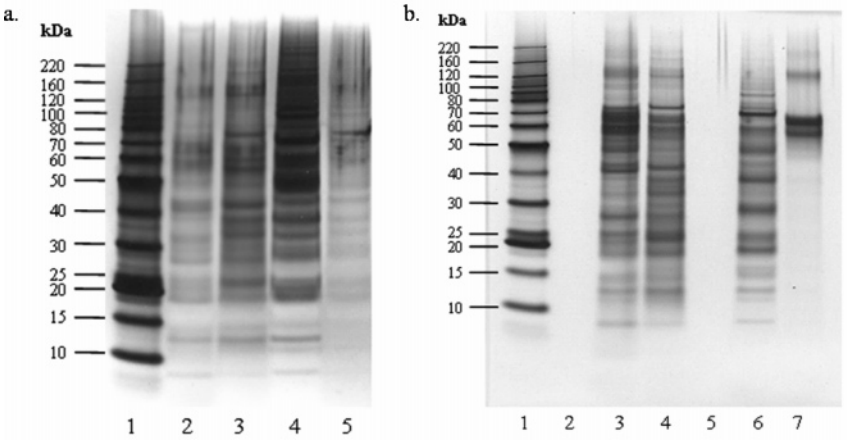

Figure 4. Comparison of lysate preparation separations. Lysates were prepared by freeze−thaw lysis (FT) or detergent solubilization in octyl β-glucoside (OG). Samples were collected as described in Methods. Released samples were concentrated with Microcon concentrator filters. Gels were silver stained. (a) Lane 1, protein ladder; lane 2, FT pre-encapsulation; lane 3, OG pre-encapsulation; lane 4, FT lysate extracted from nanoparticles; and lane 5, OG lysate extracted from nanoparticles. (b) Lane 1, protein ladder; lane 3, FT pre-encapsulation; lane 4, OG pre-encapsulation; lane 6, FT released; and lane 7, OG released.

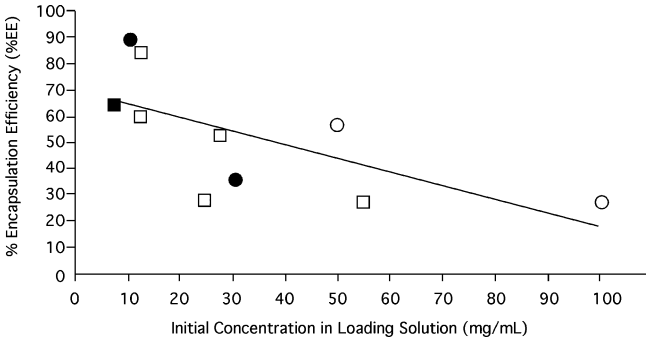

Figure 5. Effect of initial loading concentration on encapsulation efficiency. Polymer nanoparticles (80K MW) made with different loadings of FT lysates (□), OG lysate (■), pure OVA (○), and defined multiproteins (●) at various concentrations. The trend line is $y = -0.5228x + 70.185$, where $R^2 = 0.43$. $R^2 = 0.7$ for OVA samples only.

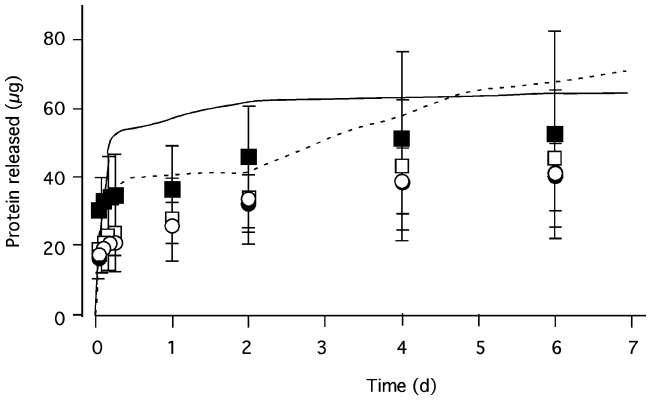

Figure 6. Release of FT lysates made from different formulations of PLGA is similar to release of single proteins. FT lysates encapsulated in 45K with 5% PVA (●), 45K with 0.5% PVA (○), 80K with 5% PVA (■), and 80K with 0.5% PVA (□). Nanoparticle samples were loaded with 55 mg/mL FT lysate and 2 mg of FITC-OVA. The total protein was detected using the BCA assay. For comparison, the release is also shown for OVA-loaded nanoparticles (80K MW with 5% PVA) loaded at 50 (- - -) and 100 mg/mL (—).

The protein banding patterns changed when the lysate preparations were encapsulated and released (Figure 4). The FT lysate gel patterns of encapsulated proteins were similar (panel a, lane 4) to those of the encapsulated OG lysate (lane 5) and to the distributions that existed pre-encapsulation (lanes 2 and 3). The distribution of protein bands from the released FT lysate (panel b, lane 6) exhibited banding patterns similar to that of the pre-encapsulated FT lysate (panel b, lane 2) with bands at 70K, 50K, 40K, 28K, 25K, 20K, and 13K, but now missing the band at 130K. The released OG preparation (Figure 3b, lane 7) was missing the lower-molecular weight proteins below 50K (lane 4) seen in encapsulated preparations. Instead, three dark bands located at 60K, 55K, and 130K formed the entire distribution on the gel (Figure 3, right, lane 7).

We explored the effect of increasing the loading concentration of cell lysate proteins on the encapsulation efficiency (Figure 5). When cell lysates were encapsulated at various initial protein loadings in 80K polymer, encapsulation efficiencies increased with a decreasing initial protein concentration in the water phase. This same trend was seen for single-protein encapsulation with the 80K MW polymer.

The pattern of the release of protein from nanoparticles with encapsulated cell lysates was the same for the two MW polymers that were tested, 45K and 80K (Figure 6). The shape of the protein release curves for nanoparticles with encapsulated cell lysate was similar to that of OVA release curves (loaded with 100 mg/mL OVA). The duration of the sustained release phase was shorter for the nanoparticles made from lysate.

To determine the encapsulation behavior of a single Ag within a lysate, we added FITC-OVA to a lysate preparation and encapsulated the mixture in nanoparticles with two different MWs, 45K and 80K. The loaded protein mixture contained 10% FITC-OVA, but the encapsulated protein

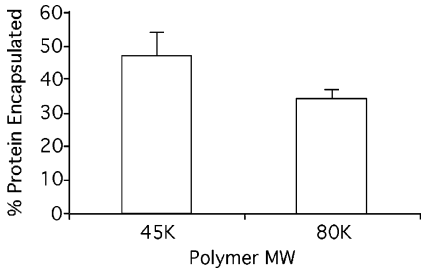

Figure 7. Percentage of total protein as FITC-OVA Ag in nanoparticles with different MW polymers. FITC-OVA was co-encapsulated with FT lysate protein, and the Ag and total protein were detected by two separate methods. The original loading concentrations of FITC-OVA and protein lysate were 50 μL of a 22 mg/mL solution and 185 μL of a 55 mg/mL solution, respectively.

contained a much larger percentage of FITC-OVA (Figure 7). OVA was readily detected in the protein mixture released from the nanoparticles (Figure 8a, lane 6) and detected with an anti-OVA antibody (Figure 8c, lane 6). OVA was also detected in the mixture of the defined protein composite after release from nanoparticles (Figure 8c, lane 7).

We also tested a known tumor-associated Ag, gp100, which was added to the cell lysate preparation and encapsulated in nanoparticles. The gp100 protein was released from the nanoparticles and readily detected via SDS−PAGE (Figure 9a, lanes 2−4) and Western blot analysis (Figure 9c, same lanes). These results indicate that tumor-associated Ags can be encapsulated and released without measurable degradation by lysate-derived contaminating proteases; in addition, the Ags are not altered by the encapsulation process.

Biological Activity of Encapsulated Ags. We used the B16 melanoma cell line because this highly aggressive and poorly immunogenic melanoma tumor cell line[13] has been used in C57BL/6 mice as the model of choice for developing vaccination protocols useful in immunotherapy of human melanoma. B16 is known to contain the murine homologues of the human tumor-associated proteins TRP 1&2 and gp100.[12] To confirm the effectiveness of nanoparticle-mediated antigen delivery, we designed experiments utilizing the melanoma-associated protein gp100 as the target Ag and naïve murine gp100-specific T cells as the readout for Ag-specific stimulation.

We found that gp100 encapsulation in nanoparticles led to superior cytokine production for both cytokines that were tested (IL-2, 10-fold increased stimulation; IFNγ, 3-fold increase), indicating nanoparticle encapsulation was associated with an increased level of production of the CTL- or Th1-associated cytokines crucial to antitumor immunity (Figure 10). In a second group of experiments utilizing the gp100-specific readout, cell lysates from B16, containing gp100, were also encapsulated into PLGA nanoparticles and compared to soluble lysates as controls. In all cases, encapsulation of the Ag preparation in nanoparticles enhanced cytokine production (Figure 10). The levels of IL-2 and IFNγ produced by T cells stimulated by DCs which had been loaded with blank PLGA nanoparticles were not significantly above the levels of cytokines produced by T cells stimulated by DCs alone (data not shown).

To determine whether encapsulation of Ag in nanoparticles led to more potent DC-based vaccines, FT lysates or FT lysates encapsulated in PLGA nanoparticles were compared

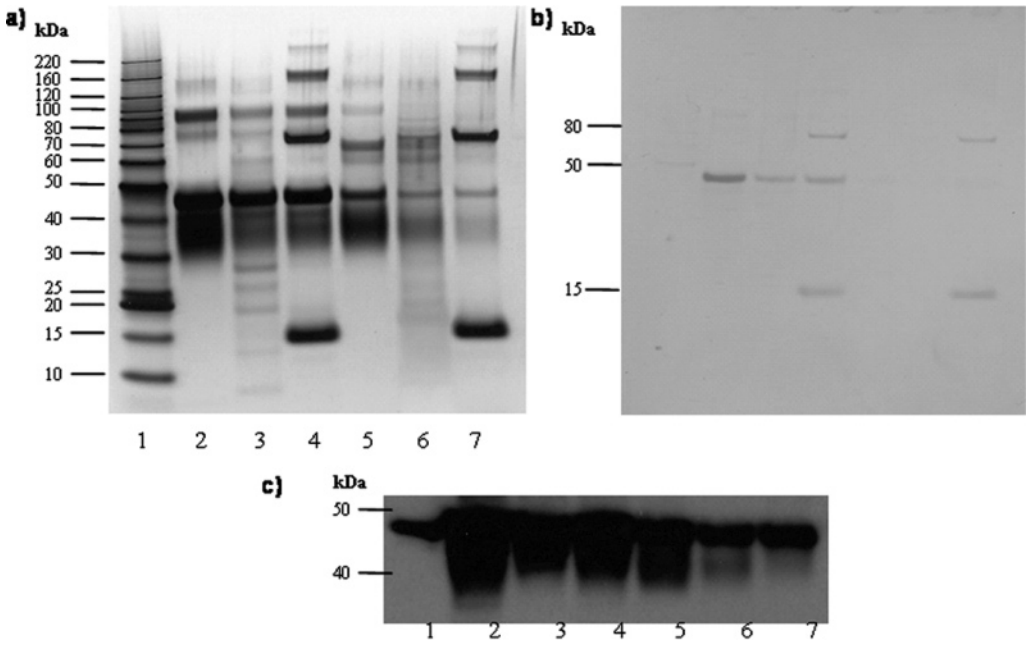

Figure 8. OVA protein alone or from complex mixtures characterized before and after encapsulation: (a) SDS−PAGE gel, silver stained, (b) Simply Blue-stained membrane after blotting gel, and (c) Western blot of membrane probed with anti-OVA antibody. Lanes 1−7: (1) benchmark ladder, (2) OVA dissolved in PBS, (3) OVA with FT lysate, (4) BSA, OVA, and LYS, (5) OVA released from nanoparticles, (6) OVA with FT lysate released from nanoparticles, and (7) BSA, OVA, and LYS released from nanoparticles.

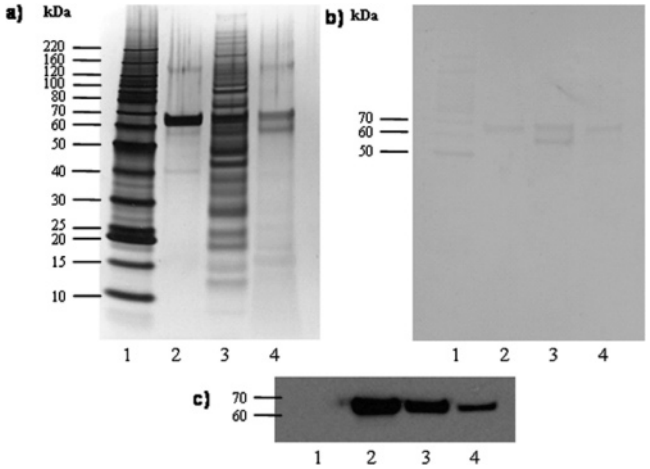

Figure 9. gp100 protein alone or within a B16 lysate characterized pre- and post-encapsulation. (a) Silver-stained SDS−PAGE gel: lane 2, gp100 protein; lane 3, FT lysate with gp100 protein; and lane 4, protein released from gp100 protein−FT lysate nanoparticles. (b) Blotted nitrocellulose gel stained with Simply Blue dye. (c) Detection of gp100 by Western blot analysis with chemiluminescent visualization. gp100 was detected in all three samples.

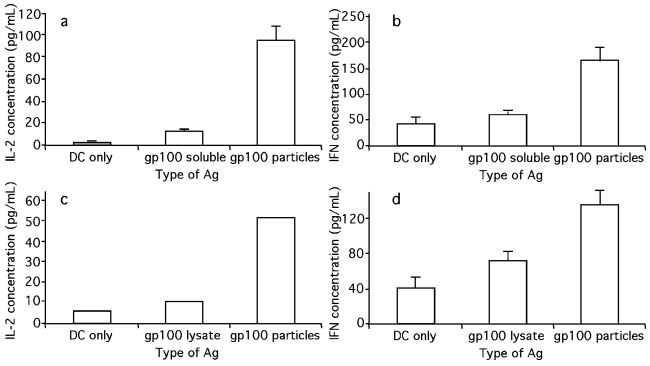

Figure 10. Enhanced stimulation of naïve gp100-specific CD8+ T cells after presentation of nanoparticle-encapsulated Ag by DC. Experiments were performed with gp100 protein (a and b) and gp100 protein within a murine B16 melanoma cell lysate (c and d). T cells were evaluated for secretion of IL-2 (a and c) and IFNγ (b and d).

for their ability to protect mice in an in vivo DC-based vaccination−challenge experiment. Here C57BL/6 mice were vaccinated with DC loaded with B16 lysates (soluble, nanoparticle-encapsulated, or controls) and subsequently challenged on the opposite flank with a lethal dose of B16, administered subcutaneously. Vaccination with nanoparticle-loaded DC provided the greatest protection against future tumor growth, with mean tumor volumes smaller than those observed with any other antigen source (Figure 11). Interestingly, when the lysate-containing nanoparticles were injected without DC, tumors actually grew faster than in the PBS-only control, suggesting that the lysate-containing nanoparticles were potentially tolerizing without DC antigen presentation.

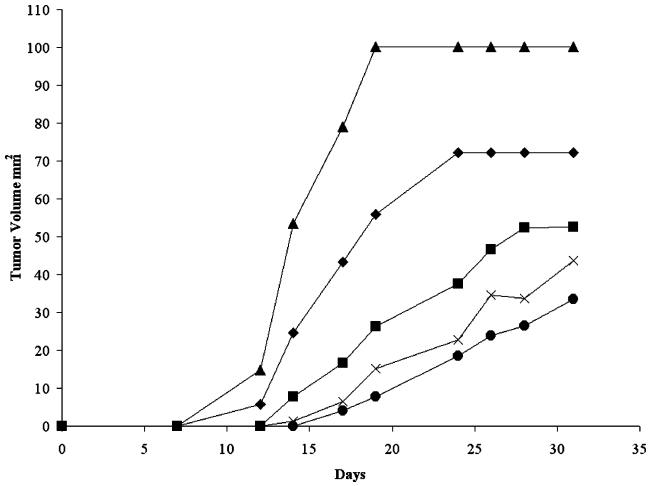

Figure 11. Encapsulation of B16 whole tumor lysate in nanoparticles leads to enhanced protection in a B16 vaccination−challenge model. After nanoparticle encapsulation, DC loading, and vaccination, the best protection from later tumor growth was associated with Ag delivery in PLGA nanoparticles. PBS (sham)-vaccinated animal (◆), animals vaccinated with unloaded DCs (■), animals vaccinated with B16 nanoparticles only (▲), animals vaccinated with DCs loaded with soluble B16 lysate (×), and animals vaccinated with DCs loaded with B16 nanoparticles (●). Eight animals were included in each experimental group. Raw data on individual animals are available as Supporting Information.

Discussion

Nanoparticles and microparticles formed from biodegradable polymers, principally PLGA and related copolymers, have long been used as vehicles for protein and antigen delivery.[14,15,16,17] In this report, we sought to create particulate delivery systems that provide (1) a small size for easy internalization by DCs, (2) sustained release of protein over 7 days, the approximate period of DC functional maturation, and (3) a high encapsulation efficiency and release capability for a range of Ag sources, including purified proteins and tumor tissue. In previous work, we showed that particles of approximately 500 nm were efficiently taken up by DCs;[3] therefore, we focused here on production of nanoparticles with diameters of <500 nm. In tailoring the properties of these particles, we were guided by previous reports which have explored the effect of fabrication variables (such as

(14) Mathiowitz, E.; Saltzman, W. M.; Domb, A.; Dor, P.; Langer, R. Polyanhydride microspheres as drug carriers. 2. Microencapsulation by solvent removal. *J. Appl. Polym. Sci.* **1988**, *35*, 755−774.

(15) Spenlehauer, G.; Spenlehauer-Bonthonneau, F.; Thies, C. Biodegradable microparticles for delivery of polypeptides and proteins. *Prog. Clin. Biol. Res.* **1989**, *292*, 283−291.

(16) Cohen, S.; Yoshioka, T.; Lucarelli, M.; Hwang, L.; Langer, R. Contolled delivery systems for protiens based on poly(lactic glycolic acid) microspheres. *Pharm. Res.* **1991**, *8*, 713−720.

(17) Krewson, C. E.; Dause, R. B.; Mak, M. W.; Saltzman, W. M. Stabilization of nerve growth factor in controlled release polymers and in tissue. *J. Biomater. Sci.* **1996**, *8*, 103−117.

polymer composition, MW, surfactant concentration, and protein concentration) on the properties of particles produced by the double-emulsion method.[16,18,19,20,21]

Overall, we found that increasing the MW of 50:50 PLGA improved the characteristics of the particles (Table 2). For example, the encapsulation efficiency for protein (%EE) increased with PLGA MW (Table 2). The increased viscosity of higher-MW polymer solutions might enhance protein encapsulation due to faster solidification in the particles.[4,22] MW has been explored as a formulation variable in particle production with a variety of polymer systems, including 75:25 PLGA,[16] poly(ϵ-caprolactone) (PCL),[23] poly(D,L-lactic acid-*co*-ethylene glycol) block copolymers (PLA-PEG),[9] and PLA.[25] In PCL, an increasing MW led to higher encapsulation efficiencies for BSA.[24] In PLA-PEG, MW did not influence %EE, perhaps due the small range of intrinsic viscosities studied (0.12−0.33 dL/g) or the hydrophilicity of the copolymer that was used.

Particle characteristics also depended on the initial protein loading, i.e., the concentration of protein in the internal aqueous phase of the double emulsion. In general, %EE decreased at higher protein concentrations (Table 2), probably due to the higher protein concentration gradient from the inner to the outer aqueous phase.[4] In PLA particles, a high initial loading also increases particle porosity, which facilitates diffusion of proteins and leads to faster release.[4] While we did not study the microstructure of our particles, we did observe that the higher protein loading concentration (100 mg/mL) produced greater burst release and more release at 14 days (Table 2 and Figure 2), features that are consistent with increased porosity. We also observed that PLGA with a MW of 45K and a protein concentration of 100 mg/mL gave a release curve compatible with our goal of gradual protein release (Figure 2). The biphasic release behavior, in which a short burst is followed by a period of linear release, may be particularly useful in delivering Ags.

We used the double-emulsion process to encapsulate mixtures of proteins, including mixtures that were derived from tumor cells. To evaluate the effects of protein mixtures on encapsulation and release, we first studied a three-protein model system (BSA, OVA, and LYS). A lower encapsulation efficiency was observed in nanoparticles made with BSA, OVA, and LYS than in any of the individual proteins (Table 3); we attribute this effect to the general decrease in encapsulation efficiency that occurs with a higher protein loading (Figure 5). OVA was released more efficiently when encapsulated as part of a protein mixture: less than 20% of OVA was released from nanoparticles containing only OVA (Table 3), whereas 100% of the protein (including abundant OVA; see Figure 3) was released from the BSA/OVA/LYS particles. In this case, the presence of other proteins appeared to facilitate the release of OVA.

Controlled release particles can also be produced from complex mixtures obtained by lysing tumor cells (Figure 6). Although we explored only a small range of protein preparation methods in this report, it is clear that particle properties depend on the method of tumor cell preparation. Melanoma cell proteins liberated from cells either through FT or with further detergent solubilization (using OG) showed slightly different banding patterns via SDS−PAGE (Figure 4), suggesting that the surfactant solubilizes proteins not extracted by FT. Particles prepared from lysates with OG did not release smaller proteins, even though these proteins were present in the loaded and encapsulated OG material (Figure 4). As far as we know, this is the first report of encapsulation of mammalian cell extracts or lysates in nanoparticles, but there are a few previous reports of encapsulation of bacterial cell extracts. When bacterial cell extracts of *Brucella ovis* obtained without the use of a surfactant were encapsulated in nanoparticles made of 75:25 PLGA or PCL, gel electrophoresis showed similar banding patterns before and after encapsulation and release.[8] Our data for FT preparation are consistent with this previous work; our results for OG lysates suggest that surfactants, while potentially liberating additional proteins for encapsulation, can make protein release less predictable. In addition, detergent solubilization of lysates prior to encapsulation would be less compatible with delivery to DCs, since the potential toxicity from surfactants could alter the effectiveness of DC-based therapies.

Ags encapsulated in particles retained their biological activity. Encapsulation of an Ag (in our case, OVA or gp100) within a mixture of proteins did not interfere with the ability of the antigen to react with an antibody (Figure 8) or stimulate dendritic cells (Figure 9). Most importantly, nanoparticles containing gp100 protein alone or gp100 co-encapsulated with FT lysate were able to stimulate gp100-

(18) Yang, Y.-Y.; Chung, T. S.; Ng, N. P. Morphology, drug distribution, and in vitro release profiles of biodegradable polymeric microspheres containing protein fabricated by double-emulsion solvent extraction/evaporation method. *Biomaterials* **2001**, *22*, 2331−2341.

(19) Tamber, H.; Johansen, P.; Merkle, H. P.; Gander, B. Formulation aspects of biodegradable polymeric microspherees for antigen delivery. *Adv. Drug Delivery Rev.* **2005**, *57*, 357−376.

(20) Cao, X.; Shoichet, M. S. Delivering neuroactive molecules from biodegradable microsphteres for application in central nervous system disorders. *Biomaterials* **1999**, *20*, 329−339.

(21) Murillo, M.; Goni, M. M.; Irache, J. M.; Arangoa, M. A.; Blasco, J. M.; Gamazo, C. Modulation of the cellular immune response after oral or subcutaneous immunization with microparticles containing brucella ovis antigens. *J. Controlled Release* **2002**, *85*, 237−246.

(22) Benoit, M. A.; Baras, B.; Gillard, J. Preparation and characterization of protein-loaded poly(ϵ-caprolactone) microparticles for oral vaccine delivery. *Int. J. Pharm.* **1999**, *184*, 73−84.

(23) Youan, B.-B. C. Influence of protein content on the physicochemistry of poly(ϵ-caprolactone) microparticles. *J. Appl. Polym. Sci.* **2006**, *101* (2), 1042−1050.

(24) Alonso, M. J.; Cohen, S.; Park, T. G.; Gupta, R. K.; Siber, G. R.; Langer, R. Determinants of release rate of tetanus vaccine from polyester microspheres. *Pharm. Res.* **1993**, *10* (7), 945−953.

(25) Engelhard, V. H.; Bullock, T. N.; Colella, T. A.; Sheasley, S. L.; Mullins, D. W. Antigens derived from melanocyte differentiation proteins: Self-tolerance. autoimmunity, and use for cancer immunotherapy, *Immunol. Rev.* **2002**, *188*, 136−146.

specific T cells to produce larger quantities of Th1-based cytokines when compared to their soluble counterparts or blank PLGA nanoparticles[3] (Figure 10). This observation provides proof of principle that whole tumor lysates, when delivered to DC in a particulate form, invoke T cell-released cytokines.

To date, only tumor lysate proteins liberated directly from a tumor by FT lysis have been used clinically in solid tumor immunotherapy outside of melanoma.[1] More than 95% of solid tumors treated worldwide are non-melanoma cancers; few defined Ags are available for these tumors. Therefore, an overwhelming need for alternative Ag delivery vehicles that expand opportunities to exploit DC vaccination exists. It is encouraging then that we were also able to produce an in vivo resistance to the growth of B16 melanoma in mice (Figure 11). Mice vaccinated with nanoparticle−tumor conjugates had the smallest tumors and the longest tumor-free durations when challenged with B16 melanoma cells. This in vivo observation is in agreement with our prior conclusions regarding an increased level of T cell stimulation following nanoparticle-mediated tumor delivery, since it is well-established that CD8+ T cells are the predominant cellular component of antitumor immune responses in this model.[25] These results confirmed, in a setting similar to human DC-based immunotherapy, that lysates encapsulated in PLGA nanoparticles were capable of stimulating more robust antitumor T cell responses than currently utilized Ag forms, as well as, inhibiting tumor growth in vivo.

Acknowledgment. We thank Elena Feshchenko and Michael P. Weiner for the generous donation of the GST fusion protein gp100. We thank Javier Lapiera for technical assistance. We thank members of the Girardi and Cresswell laboratories at the Yale University School of Medicine for technical assistance and helpful discussions.

Supporting Information Available: Raw animal data from the mouse vaccination experiment. The data represent the measurement of tumor area (square millimeters) of C57BL/6 mice postchallenge with live B16 melanoma cells at various time points. Mice were randomly assigned to treatment groups ($n = 8$) and subsequently examined for their rate of tumor growth. Mice were sacrificed when one of the following conditions was met: (1) the tumor reached a size of >100 mm^2 or (2) the tumor ulcerated and/or the animals exhibited signs of distress. Loss of mice in this way is reflected as blackening of rows in the raw data. This material is available free of charge via the Internet at http://pubs.acs.org.

MP060107E